ResearchGate

See discussions, stats, and author profiles for this publication at: https://www.researchgate.net/publication/236879950

Helium aggregates doped with alkali dimer impurities: A finite temperature study of 4HeN–Rb2(3Σu+) complexes

ARTICLE *in* COMPUTATIONAL AND THEORETICAL CHEMISTRY · APRIL 2012

Impact Factor: 1.55 · DOI: 10.1016/j.comptc.2012.03.018

CITATIONS
4

READS
35

7 AUTHORS, INCLUDING:

David López-Durán
Spanish National Research Council
32 PUBLICATIONS **285** CITATIONS
SEE PROFILE

Gerardo Delgado-Barrio
Spanish National Research Council
246 PUBLICATIONS **2,961** CITATIONS
SEE PROFILE

Franco A Gianturco
Sapienza University of Rome
448 PUBLICATIONS **6,225** CITATIONS
SEE PROFILE

All in-text references underlined in blue are linked to publications on ResearchGate, letting you access and read them immediately.

Available from: Rocio Rodríguez-Cantano
Retrieved on: 27 January 2016

Provided for non-commercial research and education use.
Not for reproduction, distribution or commercial use.

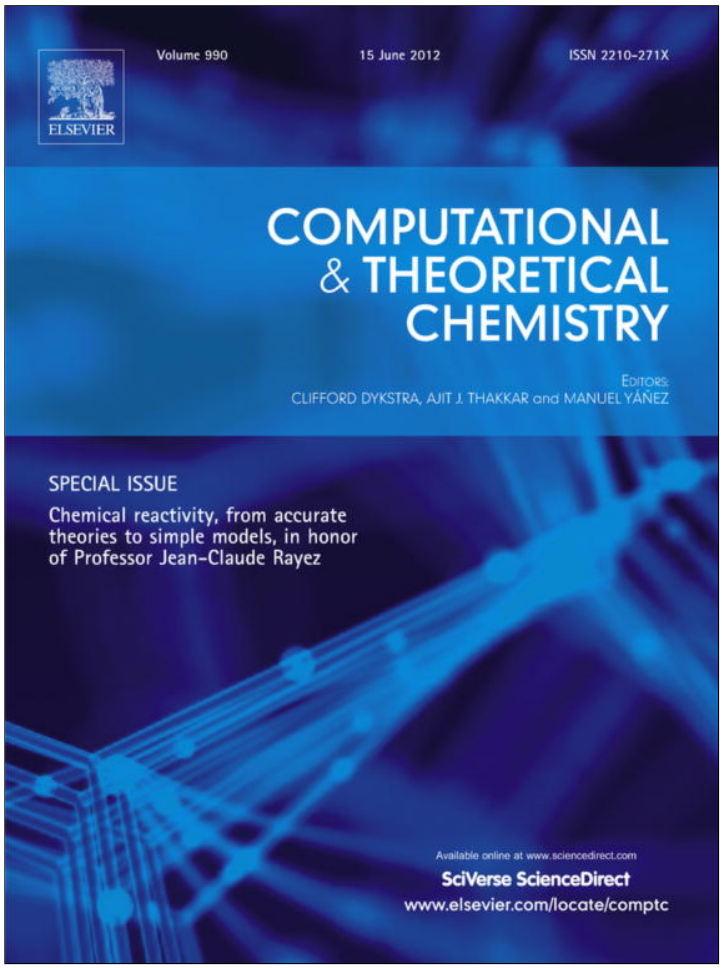

This article appeared in a journal published by Elsevier. The attached copy is furnished to the author for internal non-commercial research and education use, including for instruction at the authors institution and sharing with colleagues.

Other uses, including reproduction and distribution, or selling or licensing copies, or posting to personal, institutional or third party websites are prohibited.

In most cases authors are permitted to post their version of the article (e.g. in Word or Tex form) to their personal website or institutional repository. Authors requiring further information regarding Elsevier's archiving and manuscript policies are encouraged to visit:

http://www.elsevier.com/copyright

Author's personal copy

Computational and Theoretical Chemistry 990 (2012) 106–111

Contents lists available at SciVerse ScienceDirect

Computational and Theoretical Chemistry

journal homepage: www.elsevier.com/locate/comptc

Helium aggregates doped with alkali dimer impurities: A finite temperature study of ^4He_N—$Rb_2(^3\Sigma_u^+)$ complexes

R. Rodríguez-Cantano [a,*], D. López-Durán [a], R. Pérez de Tudela [b], T. González-Lezana [a], G. Delgado-Barrio [a], P. Villarreal [a], F.A. Gianturco [c]

[a] Instituto de Física Fundamental, IFF-CSIC, Serrano 123, 28006 Madrid, Spain
[b] Departamento de Química-Física I, Universidad Complutense de Madrid, Avda. Complutense s/n, 28040 Madrid, Spain
[c] Department of Chemistry and CNISM, University of Rome La Sapienza, Piazzale A. Moro 5, 00185 Rome, Italy

ARTICLE INFO

Article history:
Received 30 September 2011
Received in revised form 18 January 2012
Accepted 23 March 2012
Available online 13 April 2012

This work is affectionally dedicated to Jean-Claude Rayez, excellent scientist and dear friend, for his 67 birthday

Keywords:
Finite temperature
Doped helium clusters
Alkali impurity
Path integral Monte Carlo
Rubidium dimer

ABSTRACT

A path integral Monte Carlo method has been used to study small $(^4He)_N$—$Rb_2(^3\Sigma_u^+)$ complexes at low temperatures. We focus our investigation on the range 1 K $\leqslant T \leqslant$ 2 K for aggregates of different sizes containing between 10 and 40 helium atoms. The extremely weak He–Rb_2 interaction, with a shallower potential depth and a longer equilibrium bond length than in the case of the He–He interaction, favors the preference of the alkali molecular dopant to reside on the helium droplet surface. In spite of the slight perturbation introduced by the rubidium dimer, it serves like a glue for the helium host that, at a given temperature, would not exist as a pure aggregate without the presence of the dopant molecule. It is found that the stability of the clusters increases with the number of He atoms surrounding the Rb_2 dimer.
© 2012 Elsevier B.V. All rights reserved.

1. Introduction

Due to its quantum behavior ^{4}He has become crucial in the last ten years in the development of cold cryo-matrices for both atomic and molecular high-resolution spectroscopy [1], as well as for synthesizing new molecular species and clusters [2]. Helium droplets are an ideal matrix because the rare gas particles adapt softly to the dopant atom, ion or molecule (as a consequence, spectral lines are slightly modified in comparison with the free impurity), they behave electrically like vacuum (dopants may be subjected to electric fields and microwave radiation) and they are perfect for optical absorption and polarization experiments as He is optically translucent. Many of the impurities studied by Helium Nanodroplet Isolation (HENDI) [3] spectroscopy have been triplet-state spin alkali dimers [4]. These weakly bound high-spin molecules are more likely to survive than the corresponding singlet-states and are thus preferentially observed (in the latter case the release energy causes evaporation of the drop and the subsequent detachment of the alkali dimer from the cluster [5]).

Rb_2 in its ground triplet-state attached to He_N clusters, in particular, has been extensively studied, both from the experimental [6–8] and theoretical point of view [9–11]. Recently, the calculated *ab initio* points for the He—$Rb_2(^3\Sigma_u^+)$ potential energy surface (PES) have been accurately fitted to an analytical expression [10]. It consists in the simple addition of He–Rb Lennard-Jones forms, with well depth and equilibrium distance parameters depending on the orientation of the helium atom with respect to the Rb_2 axis. For ^4He_N—$Rb_2(^3\Sigma_u^+)$ complexes, considering the rubidium dimer as a rigid rotor, and representing the full PES as the sum of N He–Rb_2 interactions plus $N(N-1)/2$ He–He potentials, Diffusion Monte Carlo (DMC) energies and structural properties have been determined for small ($1 \leqslant N \leqslant 4$) [10] and larger ($2 \leqslant N \leqslant 20$) [11] clusters. In this kind of calculations, where the PES is explored millions of times, it is very important its simple but accurate analytical representation in order to maintain the computational effort within acceptable limits. In the present work we extend those studies by incorporating the effect of a finite temperature $T > 0$ K. In order to determine the influence of T on binding energies and probability distributions for different cluster sizes, Path Integral Monte Carlo (PIMC) simulations in the range $1 \leqslant T \leqslant 2$ K have been carried out. The results show the unique properties that helium aggregates manifest at low temperatures resulting from the very weak interactions with the triplet rubidium dimer.

* Corresponding author.
E-mail address: rrcantano@iff.csic.es (R. Rodríguez-Cantano).

2210-271X/$ - see front matter © 2012 Elsevier B.V. All rights reserved.
http://dx.doi.org/10.1016/j.comptc.2012.03.018

Author's personal copy

This manuscript is structured as follows: after the general simulation details in Section 2, we proceed by presenting our results and conclusions in Sections 3 and 4, respectively.

2. Simulation details

Over the past years, the PIMC method has become one of the most powerful computational tool for the microscopic description of many-body quantum systems at finite temperature. It is a numerically exact technique (within statistical and systematic errors), independent of a trial wave function, which requires only the particle mass, the temperature and the interaction potential as input parameters. A detailed review of this methodology is given in Ref. [12]. In brief, the thermal average of a quantum observable $\widehat{A}$ is given by

$$\widehat{A} = Z^{-1} \int d\mathcal{R} d\mathcal{R}' \rho(\mathcal{R}, \mathcal{R}'; \beta) \langle \mathcal{R} | \widehat{A} | \mathcal{R}' \rangle, \tag{1}$$

where $\mathcal{R} \equiv (\boldsymbol{R}_1, \boldsymbol{R}_2, \ldots, \boldsymbol{R}_N)$ is a point in the $3N$-dimensional configuration space of a N-particle system, Z is the partition function, $\rho(\mathcal{R}, \mathcal{R}'; \beta) = \langle \mathcal{R}' | e^{-\beta H} | \mathcal{R} \rangle$ the thermal density matrix of the system at low temperature T and $\beta = 1/k_B T$.

This density matrix at T is unknown, but it may be represented by a product of M matrices at a higher-temperature $T' = T \times M$:

$$\rho(\mathcal{R}_0, \mathcal{R}_M; \beta) = \int \ldots \int d\mathcal{R}_1 d\mathcal{R}_2 \ldots d\mathcal{R}_{M-1} \rho(\mathcal{R}_0, \mathcal{R}_1; \tau) \rho(\mathcal{R}_1, \mathcal{R}_2; \tau) \ldots \rho(\mathcal{R}_{M-1}, \mathcal{R}_M; \tau). \tag{2}$$

The M number defines the *beads* that constitute each *polymer* or a quantum path [13]. If M is finite we have a discrete-time path with $\tau = 1/K_B T'$ the *time step* of the path integral. For a high enough temperature T', there exist several approximations [14,15] to each density matrix of Eq. (2), $\rho(\mathcal{R}_i, \mathcal{R}_{i+1}; \tau)$. In the present quantum calculations, the *primitive* approximation based upon the Trotter formula [16], has been used:

$$\rho(\mathcal{R}_k, \mathcal{R}_{k+1}; \tau) \approx \int d\mathcal{R}' \langle \mathcal{R}_k | e^{-\tau \widehat{K}} | \mathcal{R}' \rangle \langle \mathcal{R}' | e^{-\tau \widehat{V}} | \mathcal{R}_{k+1} \rangle. \tag{3}$$

In this approximation the particles may be considered as moving freely with a small correction due to the presence of the potential $\widehat{V}$. Symmetrization of the density matrix ρ due to the bosonic character of the ^{4}He drops is not required for the studied systems at the temperatures considered [17–19].

For the present discussion we consider the following Hamiltonian $\widehat{H}$:

$$\widehat{H} = \widehat{K} + \widehat{V} = -\frac{\hbar^2}{2m} \sum_{i=1}^{N} \nabla_i^2 + \sum_{i=1}^{N} V_{\mathrm{He-Rb_2}}(\boldsymbol{R}_i) + \sum_{i<j} V_{\mathrm{He-He}}(R_{ij}), \tag{4}$$

where m is the helium atom mass, $\boldsymbol{R}_i$ is the vector joining the ith He with the center of mass (CM) of the rubidium dimer, and R_{ij} are helium–helium distances. The CM of the impurity is assumed to be fixed at the origin without either translational or rotational motion. We have described the He–He pair interaction by the well-tested Aziz potential [20], while the potential of one helium atom and the triplet rubidium dimer is analytically represented as follows [10,11]:

$$V_{\mathrm{He-Rb_2}} = d(\theta) \sum_{j=1}^{2} \left[\left(\frac{\bar{x}(\theta)}{x_j} \right)^{12} - 2 \left(\frac{\bar{x}(\theta)}{x_j} \right)^{6} \right], \tag{5}$$

where the Rb–Rb distance has been fixed at its equilibrium value of 6.35 Å, θ is the orientation of the He atom with respect to the diatomic axis, and x_j are He–Rb distances, $j = 1, 2$. The parameters $d(\theta)$ and $\bar{x}(\theta)$ are calculated by means of the following expressions:

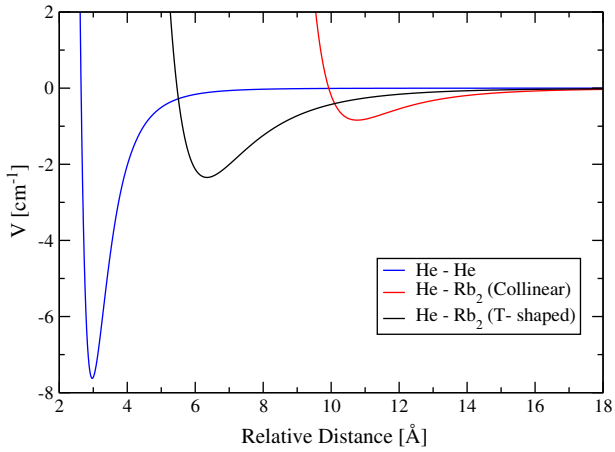

Fig. 1. He–He potential and He–Rb_2 interaction at the two indicated orientations of the He atom respect to the Rb_2 dimer axis.

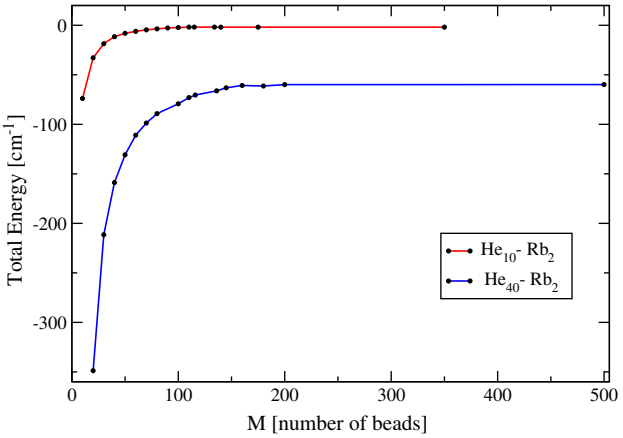

Fig. 2. Evolution of the total energy (cm^{-1}) as function of the number of beads for He_N–Rb_2 with $N = 10$ and 40 at $T = 1$ K.

$$d(\theta) = d(0) + [d(\pi/2) - d(0)] sin^{2\alpha}(\theta)$$
$$\bar{x}(\theta) = \bar{x}(0) - [\bar{x}(\pi/2) - \bar{x}(0)] sin^{2\beta}(\theta), \tag{6}$$

where the values for the coefficients, obtained by means of a fitting to previously calculated *ab initio* points for the He–Rb_2 clusters [10,11], are: $d(0) = 0.7987$ cm^{-1}, $\bar{x}(0) = 7.6044$ Å, $d(\pi/2) = 1.1730$ cm^{-1}, $\bar{x}(\pi/2) = 7.0960$ Å, $\alpha = 15.214$ and $\beta = 6.173$.

Fig. 1 displays the extreme (T-shaped and collinear) He–Rb_2 interactions, together with the He–He one, terms which drive the behavior of He_N–Rb_2 aggregates and their properties at low temperature. Although all interactions are very weak, notice the larger strength and shorter equilibrium distance of the helium-pair potential over the helium–rubidium one, independently of its angular arrangement. As result of this feature and due to the rise in temperature, the PIMC calculations have been performed with two artificial constraints in order to prevent the helium atoms from evaporation: they are confined inside a sphere centered at the diatomic CM with a radius of 30 Å, and they are not allowed to exceed a maximum distance of 15 Å from the CM of the helium drop (for $N = 10$ and $T = 1$ K, these values are reduced to 24 and 12 Å, respectively).

In our PIMC simulation, in order to estimate the value of a specific observable at a given temperature, Eq. (1), around 10^7 Monte Carlo steps have been performed after a thermalization process. The sampling in the coordinate space is performed by combining

Author's personal copy

Table 1
Total E and E/N energies (cm^{-1}) for ^4He_N–Rb_2 with $N = 10$, 20, 30 and 40 at $T = 1$, 1.25, 1.5, 1.75 and 2 K.

	T (K)				
	1	1.25	1.5	1.75	2
N = 10					
E	−1.847 ± 2.321	6.730 ± 1.938	–	–	–
E/N	−0.185 ± 0.232	0.673 ± 0.194	–	–	–
N = 20					
E	−13.195 ± 2.806	−8.712 ± 4.617	2.081 ± 2.880	13.669 ± 3.561	–
E/N	−0.660 ± 0.140	−0.435 ± 0.231	0.104 ± 0.144	0.685 ± 0.178	–
N = 30					
E	−32.833 ± 6.058	−28.526 ± 5.303	−21.158 ± 5.599	−5.071 ± 7.402	9.487 ± 8.173
E/N	−1.094 ± 0.202	−0.951 ± 0.177	−0.705 ± 0.187	−0.169 ± 0.246	0.316 ± 0.272
N = 40					
E	−60.447 ± 3.531	−49.568 ± 5.668	−40.738 ± 6.760	−28.136 ± 6.541	−11.868 ± 6.665
E/N	−1.511 ± 0.088	−1.239 ± 0.142	−1.018 ± 0.169	−0.703 ± 0.164	−0.297 ± 0.167

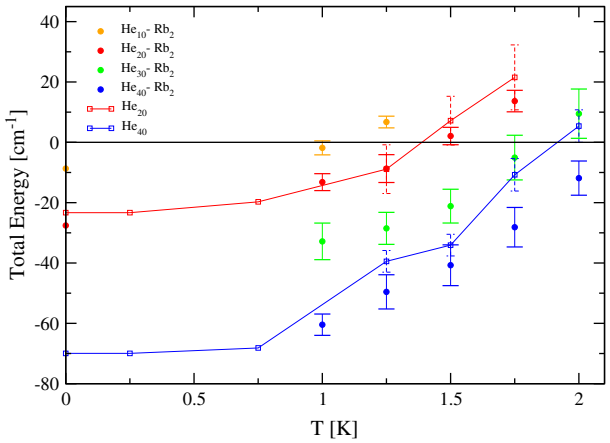

Fig. 3. Path-integral results for the total energy as a function of system temperature. Solid lines refer to $^4He_{20}$ and $^4He_{40}$ pure cluster calculations from Ref. [18] (lines are intended only to guide the eye). $T = 0$ K values correspond to DMC calculations [11].

the staging method [21] and the Metropolis algorithm [22]. The number of neighboring beads to be sampled simultaneously during the staging procedure was chosen to be $M = 8$. The kinetic energy is calculated by the virial estimator. It has been proved that, contrary to the thermodynamic estimator, the variance does not increase with the number of beads but remains constant as a function of M [23]. Individual convergence studies of the total energy (the rest of physical quantities of interest converge well before it does [24]) with respect to the number of beads M were carried out. In the present calculations we used $M = 200$ for the high-temperature density matrix. This has been sufficient to obtain converged energy results, as can be realized in Fig. 2 for clusters containing 10 and 40 He atoms at $T = 1$ K.

The simulations for each cluster size were started from the configuration which corresponds to the lowest classical potential energy structure. This arrangement was obtained by an standard evolutionary algorithm [25]. Data blocking is used to estimate statistical uncertainties [26,27].

3. Results

3.1. Energy

We have estimated total energies (E) and energy per atom (E/N) at different temperatures ranged between 1 and 2 K, for ^4He_N–Rb_2 clusters constituted by 10, 20, 30 and 40 helium atoms. Results are shown in Table 1.

As expected, for a given cluster size, the binding energy decreases with the temperature. In turn, for a fixed temperature, the cluster size is found to be a determinant factor for its stability. Thus, the binding energy increases with the number of helium atoms around the Rb_2 unit. Despite this energy may reach positive values (see Table 1), moving into an instability region, values below zero do not guarantee that the doped complex is stable: it should be also lower than the corresponding energy of the pure helium aggregate. The present PIMC energies for the He_NRb_2 clusters and available DMC/PIMC results for pure helium clusters ($N = 20$ and 40) from Ref. [18] are compared in Fig. 3.

In order to show the whole tendency with the temperature, $T = 0$ K DMC results [11] for doped clusters ($N = 10$ and 20) are also included. The range $0\ \text{K} < T \leqslant 1$ K is missing since our calculations do not incorporate exchange effects which are important at such low temperatures [19]. By looking at this figure, the stability of the present doped complexes can be easily analyzed. For $N = 10$, the cluster remains bounded up to $T = 1$ K, becoming unstable beyond. For $N = 20$, the complex is stable perhaps up to $T = 1.25$ K, but no longer exists at $T = 1.5$ K. In absence of available results for the pure aggregate, the temperature limit reaches a value of $T \equiv 1.75$ K for $N = 30$. In turn, the doped cluster with $N = 40$ remains bound in the whole temperature range analyzed. It is noticeable that, at $T = 2$ K, where the pure aggregate (including error bars) hardly exists, the doped cluster clearly remains bound. Hence, and in spite of the extremely weak perturbation induced by the presence of the dopant on the helium cluster, there is a glue effect that qualitatively transforms the character of the latter and allows its existence.

3.2. Structural properties

Both the influence of temperature and the effect of number of helium atoms on the studied system have been analyzed by means of the one- and two-particle distributions obtained varying these two parameters. For the sake of simplicity, in what follows, we will express the distance between two helium atoms as R_{He-He} and the distance between the any He atom and the Rb_2 CM is denoted by R.

Fig. 4 displays the $\cos\theta$ distribution for the extreme sizes considered, $N = 10$ and 40 at $T = 1$ K (left panel), and for $N = 40$ at $T = 1$ and 2 K (right panel). As the minimum of the well depth of the He–Rb_2 potential surface is placed at the T-shape configuration (see Fig. 1), this function shows its maximum at $\theta = \pi/2$ for all the cluster sizes and temperatures considered, becoming more peaked as N increases and/or T decreases. Consequently, the helium

Author's personal copy

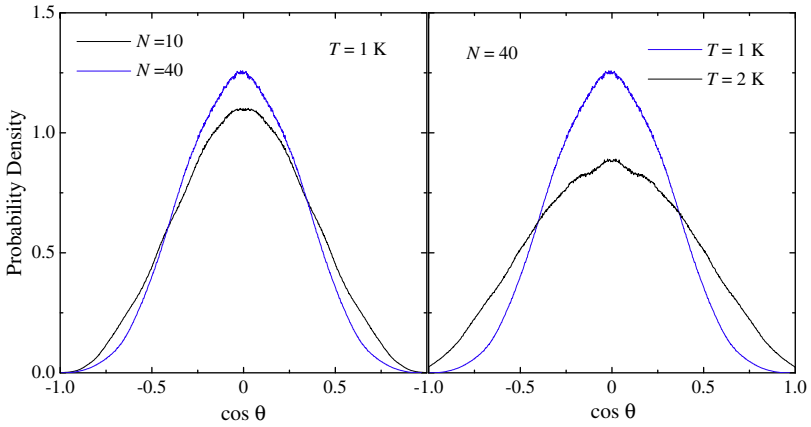

Fig. 4. One-particle angular distributions. Left panel: $T = 1$ K, $N = 10$, 40; right panel: $T = 1$, 2 K, $N = 40$.

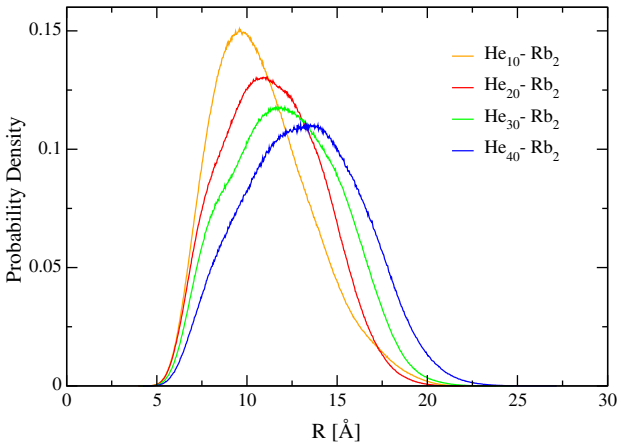

Fig. 5. One-particle radial distributions for $T = 1$ K.

adatoms are symmetrically distributed around a perpendicular region with respect to the Rb_2 axis.

Notice that the distributions of Fig. 4, directly obtained from the binning procedure of the Monte Carlo approach with no further refining numerical manipulations, are essentially symmetric with respect to $\cos\theta \sim 0$.

The radial one-particle distribution of solvent atoms at $T = 1$ K, $D(R)$, depending on the cluster size is shown in Fig. 5. These distributions look rather symmetric, and evolve moving outward as the cluster size increases. For different temperatures, we plot in Fig. 6 radial one-particle distributions of doped clusters with $N = 20$ (left panel) and 40 (right panel). In both cases, probability density profiles move outwards and spread over a broader space as T increases. However, a remarkable difference does appear depending on the bound or unstable character of the cluster: for $N = 40$, since the cluster is bound at all the temperatures, the above mentioned evolution takes place from 1 K to 2 K. On the contrary, the $N = 20$ cluster is bound at the two lowest temperatures, following the same trend, but becomes unstable at the highest temperature considered (see Fig. 3). This feature manifests in the corresponding radial distribution that *abnormally* shifts towards longer distances, falling down steeply at $R = 30$ Å as a consequence of the imposed confinement. As a matter of fact, the one-particle angular distributions which correspond to unstable clusters present irregular profiles and lose the typical symmetry around $\theta = \pi/2$ exhibited by bound clusters as shown in Fig. 4.

Consistent with the different trend of the binding energies with respect to the temperature observed in Fig. 3, the radial distributions shown in Fig. 5 manifest that the presence of a larger number of He atoms surrounding the Rb_2 impurity provides stability to the clusters, with spatially confined $D(R)$ distributions at the largest values of T considered here (2 K).

Angular two-particle distributions at $T = 1$ K for the different cluster sizes are displayed in Fig. 7, where the γ refers to the angle formed between any two He atoms with respect to the Rb_2 CM, considered the vertex of such an angle. They present a clear maximum near 1 ($\cos\gamma \sim 0$), proving that the helium atoms remain packed closely together. A gradual spreading of $D(\cos\gamma)$ is exhibited when N increases, while no significative difference is found with temperature variations, in the range considered, for a given

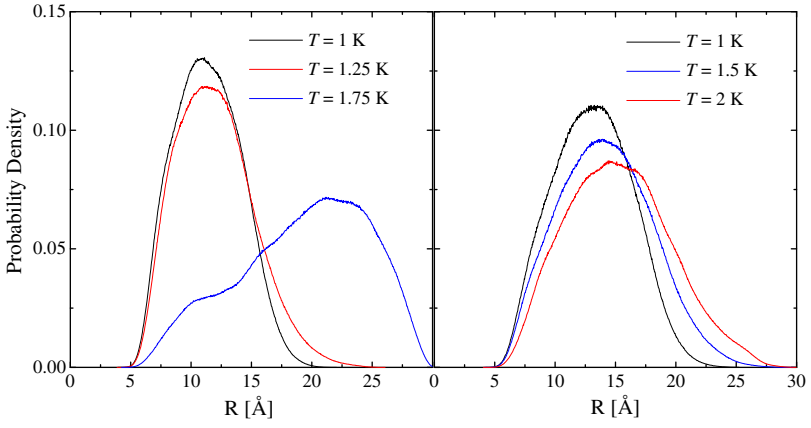

Fig. 6. One-particle radial distributions at different temperatures for $N = 20$ (left panel), and $N = 40$ (right panel).

Author's personal copy

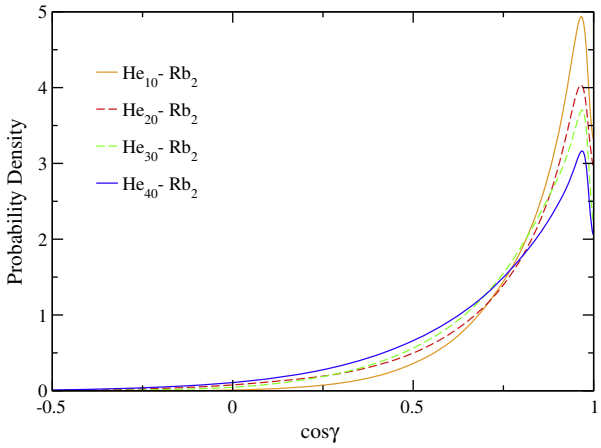

Fig. 7. $\cos\gamma$ distribution as a function of cluster size at $T = 1$ K. See text for details.

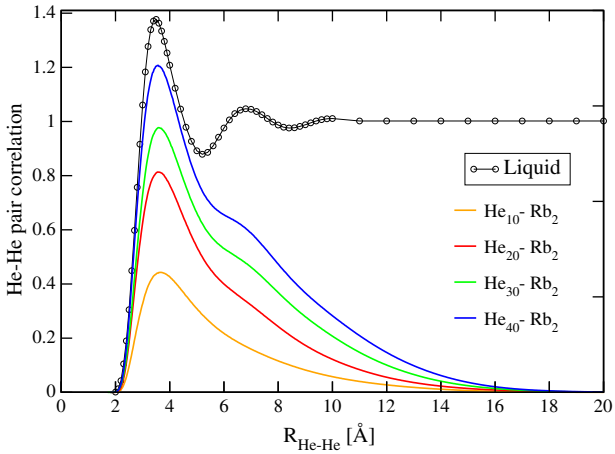

Fig. 9. PIMC evolution of the pair correlation function with the cluster size at $T = 1$ K.

drop size (not shown). This result, in combination with the large values for the distance between the He atoms, as shown in the one-particle distributions of Figs. 5 and 6, is a clear indication of the outer location of the dopant with respect of the cluster formed by the He atoms. The presence of the rare gas atoms at both sides of the Rb_2 diatom would manifest with a noticeable probability around ~ -1 for the $\cos\gamma$ distributions. Analogously a band-like structure of such atoms around the Rb_2 dopant would be accompanied by an equally distributed probability around an ample range of values for the γ angle.

A study of the dependence on the number N of the R_{He-He}- probability density reveals the existence of a magic number between 10 and 20 He atoms. Results shown in Fig. 8a display the evolution of the $D(R_{He-He})$ function from $N = 10$, with a unique flat peak, to $N \geqslant 20$, on which appear a bi-modal profile. DMC findings lead to the same conclusion for He_N–Rb_2 [11] and He_N–Cs_2 [28] composites. If temperature is enhanced, for all $N > 10$ cases (Fig. 8b for He_{40}–Rb_2 system), both cap-peaks become slightly flatter and the He–He distance distributions spread to the space. This shell-like helium atoms arrangement has an extremely high degree of delocalization, as we point out from Fig. 5, where only one peak is perceived from the $D(R)$ probability density functions.

The shoulder-plus-peak structure discussed above, can be further analyzed by means of the helium–helium pair correlation function $g_N(R_{He-He})$ calculated as [19]:

$$g_N(R_{He-He}) \propto N \times \frac{D(R_{He-He})}{R^2_{He-He}}. \quad (7)$$

As presented in Fig. 9, the pair correlation functions obtained for different number of He atoms display a double peak structure which is in agreement with the result found for the bulk at $T = 1$ K [29]. In particular the main peak observed at $\sim$3.5 Å is perfectly reproduced by our simulations for the smallest clusters, and even the secondary crest ($\sim$6.5 Å) becomes evident as N increases. As a consequence of the extremely weak interaction between the dopant and the rare gas atoms, the gross features in the experimentally observed pair distributions for bulk helium are reproduced by adding helium atoms to finite-size clusters.

4. Conclusions

In summary, we have performed finite temperature ($1 \leqslant T \leqslant 2$ K) PIMC calculations of physical properties for a rigid non-rotating alkali Rb_2 molecule attached to a ^4He_N nanodroplet ($N \leqslant 40$). Results of bounded configurations indicate that, independently of N and T, Rb_2 is sitting at the ^4He_N drop surface in a T-shaped arrangement, as would be expected due to the PES characteristics in a classical representation. Nevertheless, the distance from the impurity CM to the helium moiety (R) is function of these two parameters. For a given temperature, the larger distance is found with the maximum number of helium atoms ($N = 40$), while for a given N, as T falls, closer is the drop to the dimer.

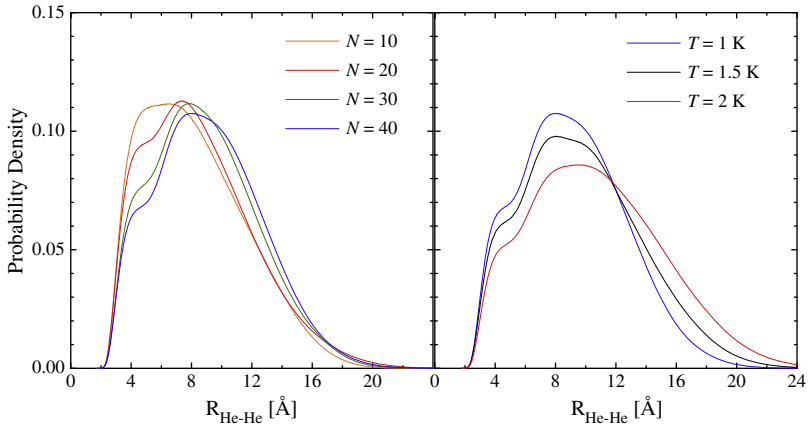

Fig. 8. Two-body radial distribution functions. Left panel (a): different cluster sizes at $T = 1$ K. Right panel (b): He_{40}–Rb_2 at temperatures between 1 and 2 K.

Author's personal copy

The addition of He atoms around the Rb_2 impurity has been found to provide stability to the clusters: On one hand, larger binding energies are obtained as N increases and, on the other hand, the radial distributions remain spatially confined at larger values of the temperature if the number of atoms is sufficiently high.

The two-body radial distributions indicate a diffuse shell-like structure on the helium sub-complex less dispersed as T is decreased, and unperturbed by the presence of their outsider dopant. Moreover, the obtained helium–helium pair correlation function tendency toward the bosonic-liquid helium one with increasing the cluster size confirms the predicted disposition in which helium atoms tend to pack themselves forming almost pure clusters.

Finally, we want to underline that further work on the title system may be required in order to include the impurity rotational degrees of freedom. Moreover, bosonic exchange symmetry is planned to be implemented in our code with the purpose of decreasing the temperature of simulation. In this sense it is worth mentioning that the dependence with the vibrational excitation of Rb_2 has been found not to play a substantial role [10,11].

Acknowledgments

We thank Centro de Cálculo (IFF, CSIC), Centro Técnico de Informática (CTI, CSIC) and Centro de Supercomputación de Galicia (CESGA) for the allocation of computer time. This work has been supported by MICINN, Grants FIS2010-18132 and FIS2011-295 96-C02-01. R.R.-C. and D.L.-D. acknowledge to the Spanish programs JAE-PREDOC, Grant No. JAE-Pre-2010–01277, and JAE-DOC, Contract Id. E-28-2009-0448699, respectively.

Appendix A. Supplementary material

Supplementary data associated with this article can be found, in the online version, at http://dx.doi.org/10.1016/j.comptc.2012.03.018.

References

[1] J.P. Toennies, A.F. Vilesov, Ang. Chem. Int. Ed. 43 (2004) 2622.
[2] O. Bünermann, F. Stienkemeier, Eur. Phys. J. D 61 (2011) 645.
[3] P. Class, G. Droppelmann, C.P. Schulz, M. Mudrich, F. Stienkemeier, J. Phys. Chem. A 111 (2007) 7537.
[4] W.E. Ernst, R. Huber, S. Jiang, R. Beuc, M. Movre, G. Pichler, J. Chem. Phys. 124 (2006) 024313.
[5] J. Higgins, C. Callegari, J. Reho, F. Stienkemeier, W.E. Ernst, M. Gutowski, G. Scoles, J. Phys. Chem. A 102 (1998) 4952.
[6] O. Allard, J. Nagl, G. Auböck, C. Callegari, W.E. Ernst, J. Phys. B: Atmos. Mol. Opt. Phys. 39 (2006) S1169.
[7] M. Mudrich, F. Stienkemeier, G. Droppelmann, P. Claas, C.P. Schulz, Phys. Rev. Lett. 100 (2008) 023401.
[8] G. Auböck, M. Aymar, O. Dulieu, W.E. Ernst, J. Chem. Phys. 132 (2010) 054304.
[9] G. Guillon, A. Zanchet, M. Leino, A. Viel, R.E. Zillich, J. Phys. Chem. A 115 (2011) 6918.
[10] R. Rodríguez-Cantano, D. López-Durán, T. González-Lezana, G. Delgado-Barrio, P. Villarreal, E. Yurtsever, F.A. Gianturco, J. Phys. Chem. A 116 (2012) 2394.
[11] D. López-Durán, R. Rodríguez-Cantano, T. González-Lezana, G. Delgado-Barrio, P. Villarreal, E. Yurtsever, F.A. Gianturco, J. Phys. Condens. Matter 24 (2012) 104014.
[12] D.M.C. Bernard Bernu, Quantum simulations of complex many-body systems: from theory to algorithms, in: J. Grotendorst, D. Marx, A. Muramatsu (Eds.), Lecture Notes, NIC Series 10, John von Neumann Institute for Computing, Julich, 2002, p. 51.
[13] D.M. Ceperley, Rev. Mod. Phys. 67 (1995) 279.
[14] L. Brualla, K. Sakkos, J. Boronat, J. Casulleras, J. Chem. Phys. 121 (2004) 636.
[15] S. Jang, S. Jang, G.A. Voth, J. Chem. Phys. 115 (2001) 7832.
[16] H.F. Trotter, Proc. Am. Math. Soc. 10 (1959) 545.
[17] D.M. Ceperley, E.L. Pollock, Phys. Rev. Lett. 56 (1986) 351.
[18] J. Boronat, K. Sakkos, E. Sola, J. Casulleras, J. Low Temp. Phys. 148 (2007) 845.
[19] R.P. de Tudela, D. López-Durán, T. González-Lezana, G. Delgado-Barrio, P. Villarreal, F.A. Gianturco, E. Yurtsever, J. Phys. Chem. A 115 (2011) 6892.
[20] R.A. Aziz, M.J. Slaman, J. Chem. Phys. 94 (1991) 8047.
[21] M. Sprik, M.L. Klein, D. Chandler, Phys. Rev. B 31 (1985) 4234.
[22] N. Metropolis, A.W. Rosenbluth, M.N. Rosenbluth, A.H. Teller, E. Teller, J. Chem. Phys. 21 (1953) 1087.
[23] M.F. Herman, E.J. Bruskin, B.J. Berne, J. Chem. Phys. 76 (1982) 5150.
[24] J.E. Cuervo, P.-N. Roy, J. Chem. Phys. 125 (2006) 124314.
[25] M. Iwamatsu, Comput. Phys. Comm. 142 (2001) 214.
[26] J. Cao, B.J. Berne, J. Chem. Phys. 91 (1989) 6359.
[27] H. Flyvbjerg, H.G. Petersen, J. Chem. Phys. 91 (1989) 461.
[28] D. López-Durán, R.P. de Tudela, R. Rodríguez-Cantano, T. González-Lezana, M.P. de Lara-Castells, G. Delgado-Barrio, P. Villarreal, Phys. Scr. 84 (2011) 028107.
[29] E.C. Svensson, V.F. Sears, A.D.B. Woods, P. Martel, Phys. Rev. B 21 (1980) 3638.